



Carbon degradation and mobilisation potentials of thawing permafrost peatlands in Northern Norway

Sigrid Trier Kjær^{1,2}, Sebastian Westermann^{2,3}, Nora Nedkvitne¹, Peter Dörsch^{1,3}

¹ Faculty of Environmental Sciences and Natural Resource Management, Norwegian University of Life Sciences,

5 NMBU, Ås, 1433, Norway

² Department of Geosciences, University of Oslo, Oslo, 0371, Norway

³ Centre for Biogeochemistry in the Anthropocene, University of Oslo, 0371, Norway

Correspondence to: Sigrid Trier Kjær (sigrid.trier.kjar@nmbu.no)

10 **Abstract.** Permafrost soils are undergoing rapid thawing due to climate change and global warming. Permafrost
peatlands are especially vulnerable since they are located near the southern margin of the permafrost domain in
the discontinuous and sporadic permafrost zones. They store large quantities of carbon (C) which, upon thawing,
are decomposed and released as carbon dioxide (CO₂), methane (CH₄) or dissolved organic carbon (DOC). This
study compares carbon degradation in three permafrost peatland ecosystems in Finnmark, Norway, which
15 represent a well-documented chronosequence of permafrost formation. Peat cores from active layer, transition
zone and permafrost zone were thawed under controlled conditions and incubated for up until 350 days under
initially-oxic or anoxic conditions while measuring CO₂, CH₄ and DOC production. Carbon degradation varied
among the three peat plateaus but showed a similar trend over depth with largest CO₂ production rates in the top
of the active layer and in the permafrost. Despite marked differences in peat chemistry, post-thaw CO₂ losses from
20 permafrost peat throughout the first 350 days in the presence of oxygen reached 67-125% of those observed from
the top of the active layer. CH₄ production was only measured after a prolonged anoxic lag phase in samples from
transition zone and permafrost, but not in active layer samples. CH₄ production was largest in thermokarst peat
sampled next to decaying peat plateaus. DOC production by active layer samples throughout 350 days incubation
exceeded gaseous C loss (up to 23-fold anoxically), whereas little DOC production or uptake was observed for
25 permafrost peat after thawing. Taken together, permafrost peat in decaying Norwegian peat plateaus degrades at
rates similar to active layer peat, while highest CH₄ production can be expected after inundation of thawed
permafrost material in thermokarst ponds.

1 Introduction

In the northern hemisphere, around 15 % of the terrestrial surface is underlain by permafrost, of which 8 - 12%
30 are permafrost-affected peatlands, covering ~1.7 million km² (Obu et al., 2019; Hugelius et al., 2020). About one
third of the carbon (C) stored in permafrost affected soils is contained in permafrost peatlands (Lindgren and
Hugelius and Kuhry, 2018), amounting to ~185 Pg C (Hugelius et al., 2020). In northern Scandinavia, peatlands
have acted as a long-term C sink in the Holocene (Panneer Selvam et al., 2017). Due to rapid global warming,
especially in Arctic regions, permafrost is projected to thaw and alter the conditions under which the C is stable,
35 thus altering the C cycle which could result in a net release of C to the atmosphere as carbon dioxide (CO₂) and
methane (CH₄) (Wang et al., 2022).



Peatlands in northern Norway are located in the sporadic permafrost zone, forming peat plateaus and palsas, i.e. peat uplands and mounds with a frozen core lifted above the water table through formation of segregation ice (Alewell et al., 2011). Peat plateaus in northern Norway have decreased in lateral extent by 33-71% from 1950 to 40 2010, with the largest change recorded in the last decade (Borge et al., 2017). In permafrost peatlands, thawing often occur abruptly by thermal erosion due to excess ice melt (Martin et al., 2021), exposing thawing permafrost peat to anoxia when inundated in thermokarst ponds. Environmental factors controlling the degradation of organic matter from thawing peat plateaus are still poorly understood. It is unclear whether the climate change driven transformation from peat plateaus to thermokarst and non-permafrost peatlands results in an overall increase of C 45 storage or whether the system is turned into a net C source (Turetsky et al., 2007; Treat et al., 2015). Understanding the mechanisms and extent of C degradation in thawing peat permafrost are therefore crucial for predicting future arctic C balances.

In this study, we determine post-thaw degradation kinetics of peat from three Norwegian permafrost peatlands ex situ and investigate their dependency on peat quality and formation history. The peat plateaus were selected to 50 represent differences in peat and permafrost age as well as in natural geographic conditions given by a sea-to-inland gradient. We incubated samples from vertical peat profiles ranging from the surface through the active layer to the mineral layer below the permafrost peat and evaluated relative C degradation potentials of permafrost peat differing in age and decomposition history. This also allowed us to investigate differences in degradability of active layer and permafrost peat which differ greatly in O₂ availability and temperature in situ (Kirkwood et 55 al., 2021; Treat et al., 2014; Waldrop et al., 2021; Panneer Selvam et al., 2017). To compare freshly thawed permafrost peat with in situ thawed thermokarst peat, we incubated additional samples from corresponding depth profiles in neighbouring thermokarst ponds.

The main objective of the study was to quantify the C degradation potentials of permafrost peat and its partitioning into CO₂, CH₄ and dissolved organic carbon (DOC). To study the influence of oxygen availability on C 60 partitioning, peat samples were incubated both initially oxically and throughout anoxically for up to 350 days. To explore the role of microbial growth for C degradation and mobilisation, a parallel set of samples was incubated for 96 days as stirred soil slurries, which eliminates diffusional constraints for substrate availability and microbial growth. To compare CO₂ and CH₄ production potentials along a thaw gradient, additional incubations were carried 65 out with recently thawed peat material obtained from shallow thermokarst depressions adjacent to two of the peat plateaus.

2 Materials and Methods

2.1 Site description

Three peat plateaus in the sporadic permafrost zone of Finnmark, northern Norway, were selected along a climatic gradient spanning from the coastal site Lakselv with maritime climate to the more continental sites Iškoras and 70 Áidejávri (Table 1). Iškoras and Áidejávri are situated on the Finnmarksvidda, a 22 000 km² plateau with elevations of 300 to 500 m a.s.l. At Iškoras, the peat development started around 9200 cal. yr. BP (Kjellman et al., 2018), while the peatland age at Áidejávri is unknown. However, the general timing of peat development is likely similar to that at the Iškoras site. The peatland at the coastal site Lakselv developed around 6150 cal. yr. BP, after the site had emerged from the adjacent fjord due to postglacial land heave. Permafrost formation for



75 Iškoras started during the Little Ice Age, with radiocarbon dates from a single core suggesting permafrost formation around 800 cal. yr. BP while formation for Lakselv occurred later around 150 cal. yr. BP (Kjellman et al., 2018). The peatlands in Lakselv are situated under the marine limit and the total column integrated C content is smaller than at Iškoras (Kjellman et al., 2018). The soils at the three peat plateaus are characterised as histosols (IUSS Working Group WRB 2014).

80 **Table 1: Location and characteristics of the three study sites. The mean annual air temperature (MAAT) and mean annual precipitation (MAP) for period 1991-2020 are from the closest meteorological station (Šihččajvri for Áidejávri, Čoavddatmohkki for Iškoras, Banak for Lakselv) and were obtained from the Klimaservicesenter (2021). Differences in altitude were corrected using a standard lapse rate of $-0.65^{\circ}\text{C}/100\text{ m}$.**

	Áidejávri	Iškoras	Lakselv
Coordinates	68°44'59" N 23°19'06" E	69°20'27" N 25°17'44" E	70°7'14" N 24°59'47" E
Elevation (m a.s.l.)	398	381	50
MAAT ($^{\circ}\text{C}$)	-2.0	-1.9	+1.4
MAP (mm)	478	433	392

85 2.2 Field sampling

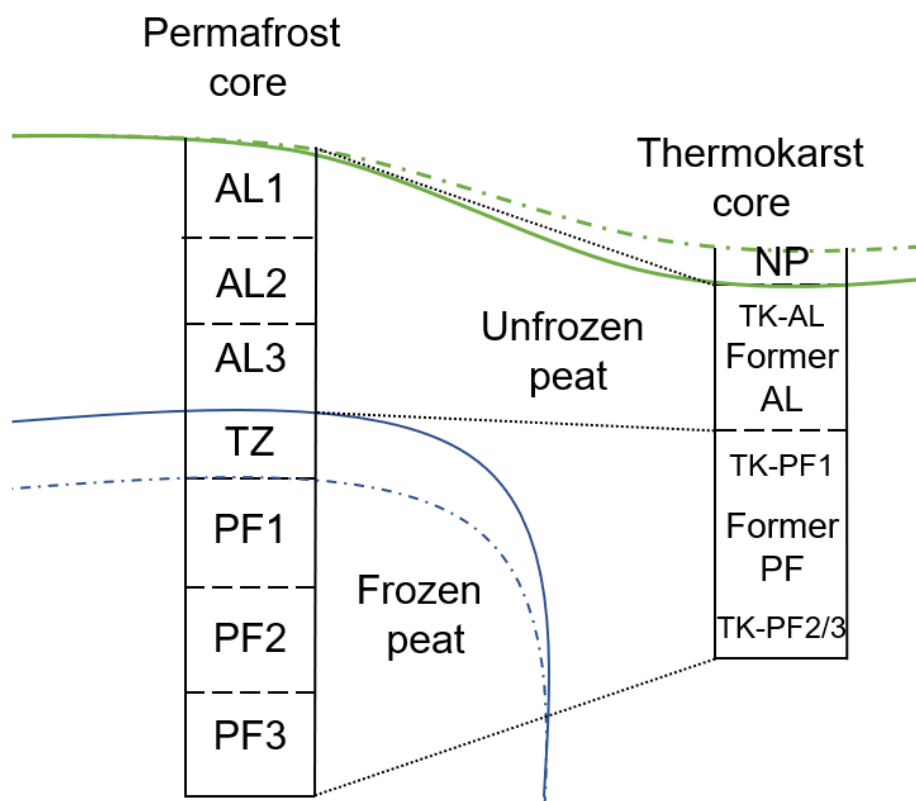
Intact cores from the permafrost-underlain peat plateaus were collected in September 2020 at the time of maximum active layer depth. The active layer (AL) was sampled using a cutting tool and a small shovel. Each core was divided into three depth layers denoted as active layer (AL), transition zone (TZ, i.e., the top of the frozen layer, which is likely to thaw occasionally) and permafrost (PF) as shown in Fig. 1. For two of the three
90 cores a fourth, mineral layer, was sampled below the peat. All active layer samples were kept cool until placed in a refrigerator at 3.8°C ($\text{SD}=0.47^{\circ}\text{C}$) in the laboratory. At the time of sampling, the active layer depth was 0.6 m at Iškoras and Lakselv and 0.5 m at Áidejávri. The frozen TZ and PF cores were sampled using a steel pipe (outside diameter 38 mm, inside diameter 30 mm) that was hammered vertically in ~ 5 cm increments into the frozen peat. A paper towel was pushed through the pipe between each sample and tools used for handling samples
95 were wiped with disinfectant to minimise cross-contamination between samples. Incremental coring was continued until reaching the mineral soil below the peat. The total thickness of the organic core (active and frozen peat layers) was 1.67 m at Iškoras, 1.04 m at Áidejávri and 0.85 m at Lakselv. Sub-samples of the core (~ 5 cm in length) were transferred to 50 ml centrifuge tubes, which were immediately sealed by a screw cap and placed into a freezing box kept below 0°C until being transferred to a -20°C freezer on the same day. The samples were
100 shipped frozen to the laboratory, where they were kept at -17.8°C ($\text{SD} = 0.39^{\circ}\text{C}$). To facilitate comparison between permafrost cores from different sites, the samples were assigned to seven operational layers according to their vertical structure, consisting of (from top to bottom) three samples from the active layer (AL1, AL2, AL3), one from the transition zone (TZ) and three from the permafrost layer (PF1, PF2, PF3). The absolute depth of the operational layers differed across the three permafrost cores (table S1).

105 Thawed peat material from thermokarst depressions adjacent to the peat plateaus was sampled in September 2021 and transferred to the lab for a 96-day incubation (see below) to study the C degradation potential of recently thawed and inundated peat material. Using orthophotos from annual drone overflights, the time of thawing was estimated to 2017/2018 for Iškoras (Fig. 2, similar to Martin et al. (2021)) and to before 2003 (from earliest available orthophoto in norgebilder.no, see Fig. 3) for Áidejávri. Visual inspection of the thermokarst cores



110 allowed to distinguish the more decomposed former active layer peat (TK-AL) from the former permafrost peat
(TK-PF1 and TK-PF2/3) below (Fig. 1), so that samples corresponding to the layers distinguished in the
permafrost cores (table S2) could be taken. In Iškoras, the former peat plateau surface was submerged under 20
cm of standing water, while a fresh peat layer had formed on top of the submerged peat plateau surface at the
Áidejávri site.

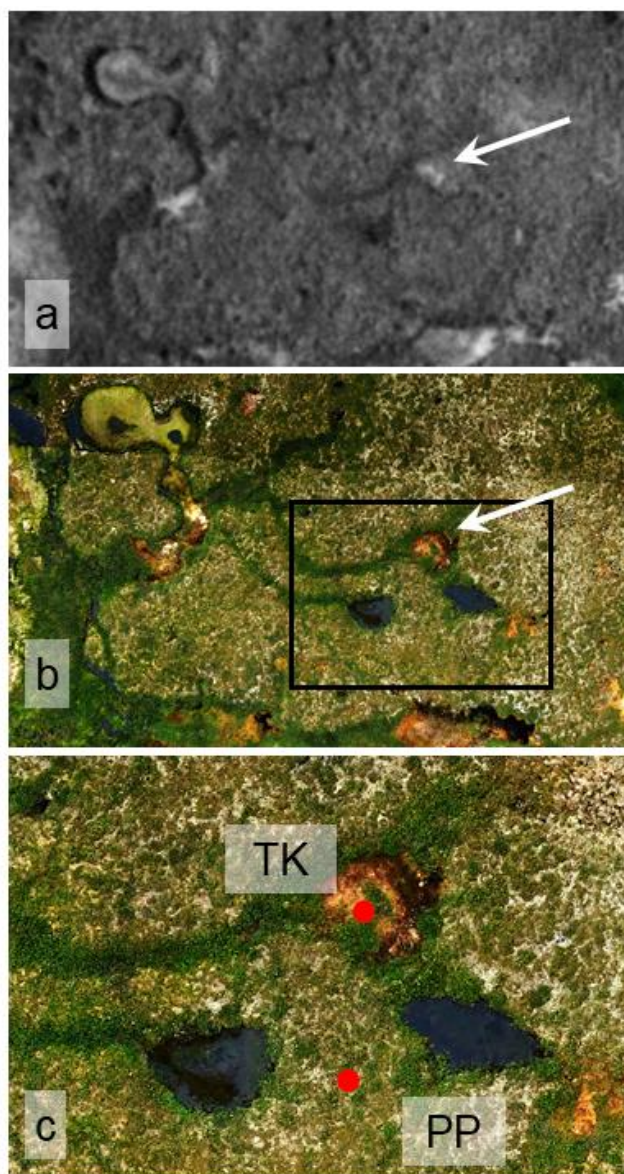
115



120 **Figure 1: Schematic drawing of permafrost and thermokarst core. The green line indicates the surface, while the green dashed line indicates growth of new peat. The blue line shows the permafrost at sampling time. The blue dashed line is the maximum thaw depth which can be occasionally thawed. AL = active layer, TZ= transition zone, PF = permafrost, TK = thermokarst, NP = new peat (i.e. accumulated following thaw, only at Áidejávri).**



125 **Figure 2:** Aerial images of the Iškoras sampling site. Top: 2015 orthophoto from a drone survey (scene width 100m), with red dots showing the locations of peat plateau (PP) and thermokarst (TK) cores sampled in 2020 and 2021, respectively. Bottom four: magnification of black rectangle for repeat orthophotos from 2015-2018, showing the initially intact peat plateau edge collapsing in a shallow thermokarst pond from where thermokarst samples were taken in 2020.



130 **Figure 3:** Aerial images of the Áidejávri sampling site; a) 2003 aerial image from norgebilder.no; b) 2018 orthophoto
135 from a drone survey; scene width a, b: 130m; c) magnification of black rectangle in b, with red dots showing the
locations of peat plateau (PP) and thermokarst (TK) cores; white arrow pointing to drained thermokarst pond visible
in both 2003 and 2018 imagery.

2.3 Stable isotope signatures and elemental analysis

135 Elemental analyses were performed on freeze-dried, homogenized samples using an IPC-MS (Agilent
Technologies 8800 ICP-MS Triple Quad) and ICP-OES (PerkinElmer FIMS). Freeze-dried samples were
decomposed using ultrapure concentrated HNO₃ (ultraCLAVE, Milestone). Traceability and accuracy of the



elemental analysis were ensured by including standards of known elemental composition (NCS ZC73013, NCS DC73349, Peach Leaves-1547, Pine Needles-1575 and River Sediment-LGC6187).

140 Contents of C and N and their natural ^{13}C and ^{15}N abundances were analysed using a flush combustion elemental analyser (Thermo EA 1112 HT O/H-N/C) coupled through a ConFlow3 interface to an isotope ratio mass spectrometer (Thermo-Finnigan Delta Plus XP). Isotope values were calibrated against certified reference materials (IAEA-N1, IAEA-CO8) and are expressed in delta (δ) notation relative to VPDB and atmospheric N_2 , respectively. To compare C content with organic matter content, loss on ignition was measured at $550^\circ\text{C} \pm 25$ with samples dried at 60°C overnight.

145 **2.4 Incubation set-up**

Incubations were set up in batches, studying one complete core of each site at a time without technical replication. Each permafrost core was divided into seven layers (Fig. 1, table S1) and the thermokarst core was divided into three or four layers from which four samples each were prepared. Each sample was divided into four portions which were placed in 120 ml serum bottles and capped with crimp-sealed Butyl septa. Frozen core samples (from
150 TZ and PF layers) were divided lengthwise while being frozen to minimise gas release. To remove gases released during sample preparation and to minimise exposure to O_2 during thawing, the bottles were placed on ice and washed with Helium 6.0 (He) using an automated manifold alternately evacuating and filling the headspace 7 times. Helium overpressure was removed before placing the bottles into a temperature-controlled cabinet at 3.8°C for overnight thawing. Headspace gas concentrations were determined after ≥ 20 h thawing.

155 After controlled thawing in He and measuring gas release, the four replicate bottles for each sample were assigned to different treatments: two bottles were kept as ‘loose peat’ at natural moisture content, while the peat in the other two bottles was dispersed in 52 ml of ultra-distilled water (3.8°C) by magnetic stirring, creating ‘peat slurries’. The slurries were stirred for one hour to fully disperse the peat, whereafter the peat material was allowed to settle, and 2 ml supernatant were sampled with a syringe to measure pH and DOC concentration. pH was measured using
160 a HACH HI70 pH meter, before centrifuging the aliquot at 10,000 G for 10 minutes and filtering it through a $0.45\ \mu\text{m}$ filter (Sterile Syringe Filter with polyethersulfone membrane, VWR International) for analysing water-extractable DOC by a Total Organic Carbon Analyser (TOC-V, Shimadzu, Japan). Hereafter, one bottle of each set (loose and slurry) was washed with He as described above to create anaerobic conditions, while the other two were washed with a He/O_2 (80/20) mixture to create initially aerobic conditions.

165 **2.5 Incubation experiments**

All bottles, both the loose and the continuously stirred peat suspensions were incubated in a temperature-controlled water bath at 10°C , using an incubator with automated gas analysis (Molstad et al., 2007; Molstad et al., 2016). The incubator consists of a temperature-controlled water bath with submersible stirring boards holding up to 44 serum bottles (120 ml) and is placed under the robotic arm of an autosampler (GC-Pal, CTC) which
170 repeatedly pierces the septum of the bottles with a hypodermic needle and pumps ~ 1 ml via a peristaltic pump (Gilson 222XL) to a multi-column, multi-detector gas chromatograph (Agilent 7890A) equipped with an automatic sample admission system. Upon injection, the peristaltic pump is reversed, and sample gas not injected onto the columns is pumped back to the bottle together with He, maintaining the pressure in the bottles at ~ 1 atm. The GC has two columns, a poraplot Q column to separate CH_4 , CO_2 and N_2O from bulk air and a Molesieve



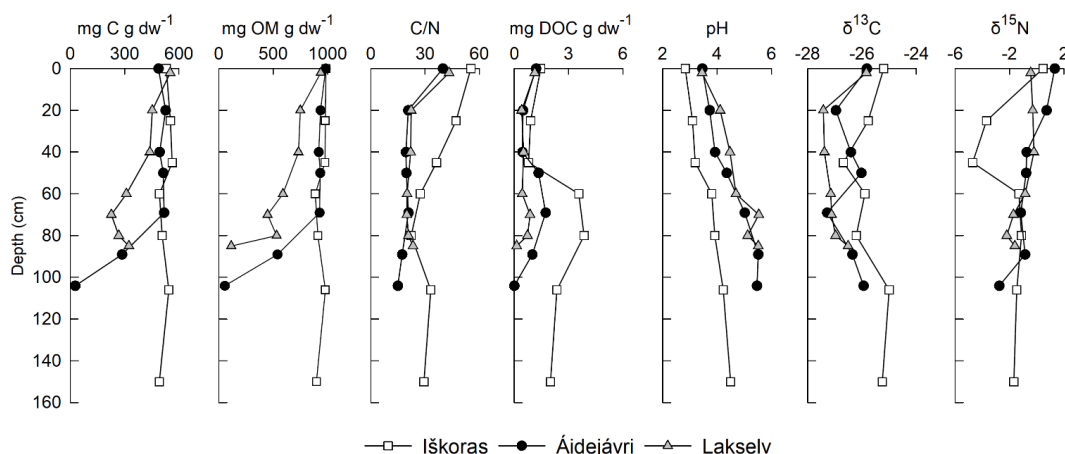
175 column to separate O₂+Ar from N₂ and three detectors (TCD, FID, ECD) for simultaneously determining O₂, CO₂,
N₂, CH₄, and N₂O concentrations. Dry bottles with standard mixtures of known concentrations (AGA, Norway)
were included into the measurement sequence for calibration and for evaluating the dilution resulting from back-
pumping He after each sampling. He-filled bottles were included to evaluate leakage of O₂ into the measurement
system.

180 Headspace gas concentrations were monitored every 4.5 h for 413-450 h (~17-19 days) for permafrost cores and
180 h (~7 days) for thermokarst cores to investigate post-thaw gas kinetics in detail. Thereafter, the bottles were
transferred to a temperature-controlled cabinet adjusted to 9.7°C (SD=0.04), where the incubations were
continued without stirring. The slurries were shaken at least once a week, after which headspace samples were
retrieved manually for off-line gas chromatography. After about one month, the measurement frequency was
185 decreased to biweekly until 96 days of incubation when incubation of slurries and thermokarst ended. Loosely
packed permafrost core samples continued incubation at 10°C until 350 days after thawing, sporadically
measuring headspace concentrations (after ~10.5 months and ~1 year). The measured gas kinetics for CO₂, CH₄,
O₂, and N₂O were corrected for dilution and leakage as described in Molstad et al. (2007). A student's t-test with
two tailed distribution and two sample unequal variance was used to evaluate differences in peat characteristics
190 among the sites.

3 Results

3.1 Peat characteristics

The peat plateau at Iškoras featured the highest C content among the three studied permafrost cores, with little
variation throughout the peat profile (491-552 mg C g dw⁻¹, Fig. 4). Permafrost cores from Áidejávri and Lakselv
195 had similar C contents in the active layer (439-551 mg C g dw⁻¹) but held less C in the permafrost. Organic matter
(OM) content mirrored C content, except for the deep permafrost (PF3) at Lakselv which indicated high
concentration of inorganic C in this layer (Fig. 4). Other layers showed no indication of inorganic C and C contents
are henceforth referred to as organic C (OC). The permafrost core from Iškoras had the highest C/N ratios
irrespective of depths, with the highest ratio in the top active layer (AL1) gradually decreasing with depth.
200 Áidejávri and Lakselv also featured the highest C/N ratios in AL1, below which they decreased more strongly
throughout the active layer, while being stable throughout the permafrost zone. DOC extracted 20 h after thawing
was highest in samples from the transition zone and from the top of the permafrost zone, with values at Iškoras
clearly exceeding those at Áidejávri and Lakselv (P<0.019). pH increased with depth at all three sites and was
significantly lower (P<0.009) at Iškoras compared to the other two permafrost cores. The permafrost core from
205 Lakselv was most depleted in ¹³C, whereas Iškoras and Áidejávri showed more variable δ¹³C values with depth.
As with δ¹³C, the δ¹⁵N values were highest in the top layer (AL1) and decreased throughout the active layer, most
so at Iškoras, and least so at Lakselv.

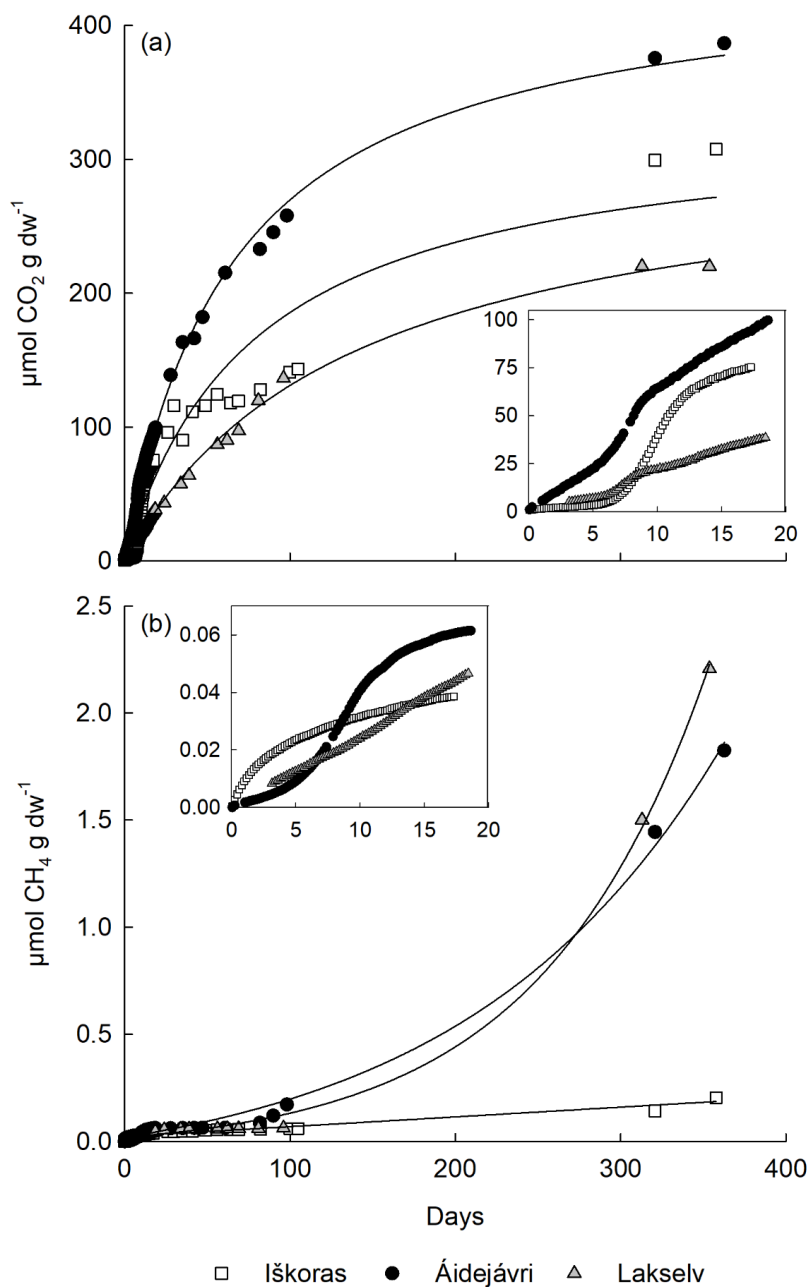


210 **Figure 4: Depth profiles of geochemical variables in permafrost cores at Iškoras, Áidejávri and Lakselv. Shown are (from left to right) carbon content (mg C g dw⁻¹), organic matter content (mg OM g dw⁻¹), carbon to nitrogen ratio (C/N), dissolved organic carbon (mg DOC g dw⁻¹), pH, and isotope signatures of carbon ($\delta^{13}\text{C}$) and nitrogen ($\delta^{15}\text{N}$). The deepest layer at Áidejávri and Lakselv were affected by mineral soils. The thaw depths at the coring location were 60 cm (Iškoras and Lakselv) and 50 cm (Áidejávri).**

215 3.2 Gas kinetics

The initial gas formation throughout the first 20 days revealed clear kinetic differences between sites and depths in permafrost cores as showcased in Fig. 5 (see also table S3 and S4). CO₂ production kinetics were most dynamic for Iškoras (TZ) showing exponential product accumulation (insert in Fig. 5a). Áidejávri (PF1) and Lakselv (PF2) also showed exponential increases in CO₂ accumulation for the permafrost layers, but to a much smaller degree (Fig. 5a; table S3). CO₂ production at all sites and depths showed a tendency to level off over time.

220 Conversely, except for Áidejávri, CH₄ accumulation was small and curve-linear during the first 20 days but increased after ~100 days in Lakselv and Áidejávri samples. During the first 96 days of the incubation, all Iškoras PF and TZ samples displayed CH₄ kinetics as shown in Figure 5b, with apparent initial CH₄ production levelling off over time no matter whether the samples were incubated stirred or unstirred, oxically or anoxically (Fig. S1), suggesting that initial CH₄ release was not due to methanogenesis. This was further supported by the higher initial CH₄ release from Iškoras samples compared to Áidejávri during the first 20 hours of thawing (table S6). In contrast, gas kinetics in samples from Áidejávri showed exponential CH₄ accumulation in TZ, PF1 and PF2 layers during the first 19 days, indicating methanogenesis (Fig. 5b, table S4, Fig. S1). After about 80 days CH₄ production increased in PF and TZ samples from Áidejávri which continued throughout the incubation. Lakselv 225 featured less CH₄ production in the beginning of the incubation which, however, increased greatly during the last part of the incubation, resulting in greater final CH₄ accumulation than in samples from Áidejávri or Iškoras (Fig. 5b). N₂O kinetics (production and uptake) were observed but accumulated amounts were minute and are not reported here.



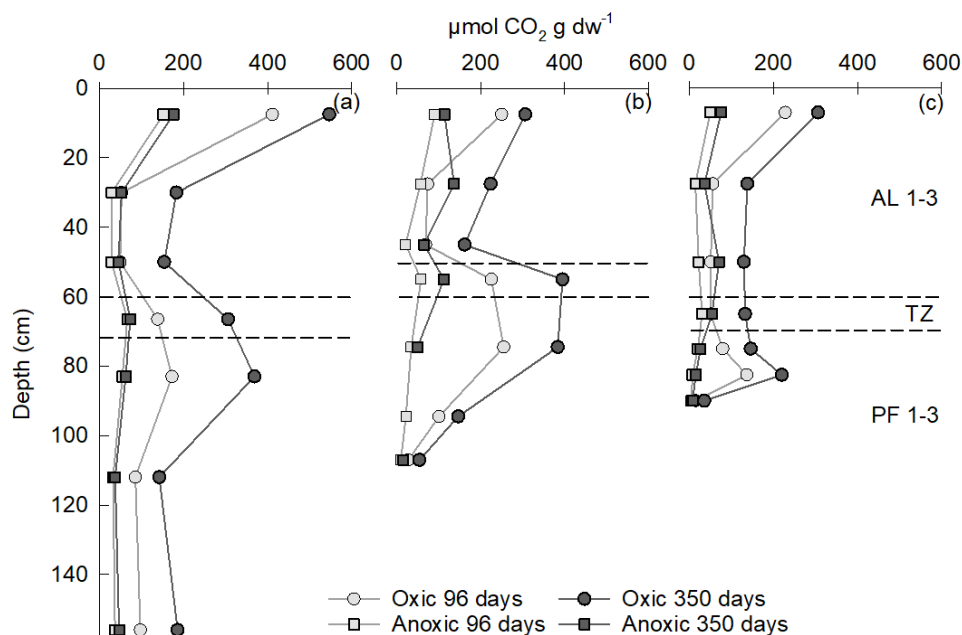
235 **Figure 5: Kinetics of CO₂ and CH₄ release from permafrost core samples (loosely packed) from layers with highest production at Iškoras (TZ), Áidejávri (PF1) and Lakselv (PF2). Initial data for Lakselv are missing due to instrument failure. (a) CO₂ accumulation of initially oxic peat throughout 350 days with fitted hyperbola ($f = a \cdot x / (b + x)$). (b) CH₄ accumulation of anoxically peat throughout 350 days fitted to a polynomial equation ($f = y_0 + a \cdot x + b \cdot x^2$).**



3.3 Cumulative CO₂ production

240 When expressed as cumulative CO₂ production over 96 days, the AL1 layers of all three permafrost cores showed
largest accumulation under oxic conditions (Fig. 6). Cumulative CO₂ production decreased strongly with depth
throughout the active layer, before increasing again in the TZ and reaching a secondary maximum in the upper
permafrost layer. Maximum CO₂ production of PF peat after 96 days accounted for 42, 102 and 60% of the CO₂
production observed in the top of the active layer (AL1) at Iškoras (PF1), Áidejávri (PF1) and Lakselv (PF2),
245 respectively, indicating that oxic post-thaw respiration of permafrost peat can reach values comparable to those
of the surface layer with fresh litter input. Across the three sites, PF peat at Lakselv accumulated least CO₂.
Incubating samples beyond 96 days revealed a gradual decrease in CO₂ production in all layers of all sites (Fig.
5a), which also coincided with reduced, and in some layers depleted, oxygen (Fig. S5, S6 and S7). However, AL
and PF top samples of the oxic treatment showed the largest relative increments in cumulative CO₂ production
250 from 96 to 350 days. After 350 days, CO₂ accumulation of PF samples from Iškoras (PF1) reached 67 % of that
of AL1, Áidejávri (PF1) 125 % and Lakselv (PF2) 72 %. CO₂ production was greatly reduced in the absence of
O₂, irrespective of depth and incubation time (Fig. 6).

In general, there was little effect of stirring on the decomposition irrespective of O₂. The incubation as constantly
agitated slurries had little effect on CO₂ production throughout the first 96 days even in the presence of O₂ (Fig.
255 S3), indicating that peat degradation was little controlled by matrix effects or diffusional constraints. However,
due to the addition of water and decrease in headspace volume, there was overall less O₂ available in slurried peat
than loosely packed peat, which likely limited oxic respiration.



260 **Figure 6: Cumulative CO₂ production over depth during 96 and 350 days in loosely packed permafrost core samples.** (a) Iškoras, (b) Áidejávri and (c) Lakselv. The depth indicates the average depth of the incubated sample. Stippled lines indicate thaw depth at sampling and the location of the transition zone (TZ). Anoxic PF2 for Áidejávri could not be measured after 96 days due to leakage.



CO₂ production in thermokarst cores (Iškoras and Áidejávri) was in the same order of magnitude as the permafrost cores (table 2).

265

Table 2: Comparison of CO₂ accumulation (96 days) in loose oxic incubations of permafrost and thermokarst core samples from Áidejávri and Iškoras. The different layers of the thermokarst core are compared to corresponding layers in the permafrost core (AL1, PF1 and PF2/PF3) as shown in Fig 1. PF2 was used as the deep permafrost sample at Áidejávri because of mineral soil in PF3. For absolute depths, see table S1 and S2.

μmol CO ₂ g dw ⁻¹ 96 days ⁻¹						
Permafrost core			Thermokarst core			
	Iškoras	Áidejávri		Iškoras	Áidejávri	
			New peat		616	
AL1	411	250	TK-AL	177	241	
PF1	173	255	TK-PF1	40	62	
PF2/PF3	97	101	TK-PF2/3	92	85	

270

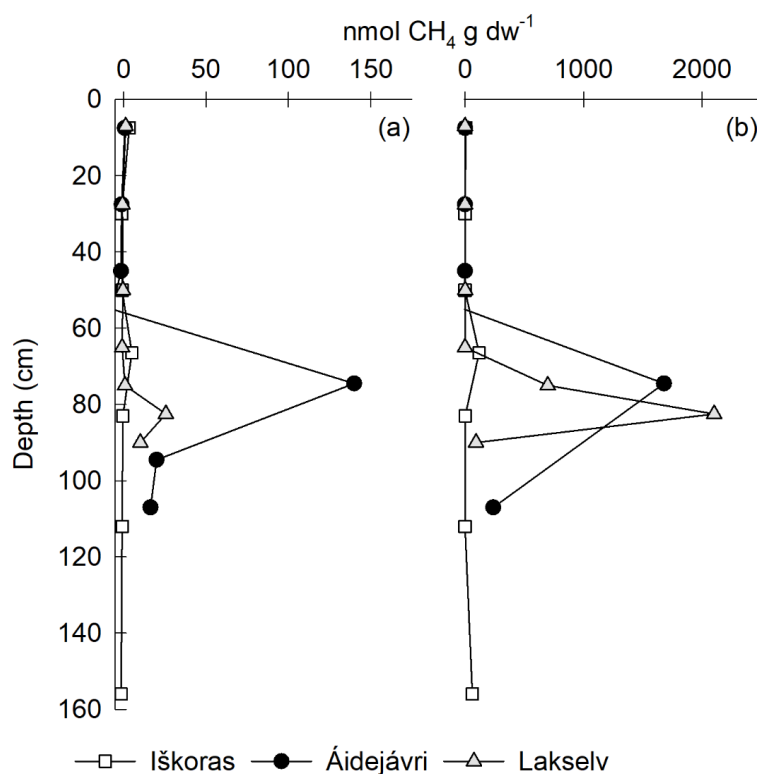
3.4 Methane release and production

In the permafrost cores, significant CH₄ production was only observed in TZ and PF samples despite prolonged anoxic incubation of samples from all depths (Fig. 7). Methane production after 96 days was up to 4 orders of magnitude smaller than CO₂ production on a C basis. Yet, while CO₂ production slowed down over time, CH₄ production increased indicating that methanogenesis in thawing PF peat was stimulated by extended periods of anoxia. Over 350 days, the anoxic CH₄-C accumulation at Lakselv (PF2) reached 38.6 % of its CO₂-C accumulation, while the corresponding values for Áidejávri (PF1) and Iškoras (TZ) were 9.2 % and 0.4 %, respectively.

275

As with CO₂, suspending and constantly stirring the peat slurry had little effect on CH₄ production within the first 96 days (Fig. S2). Much to the contrary, CH₄ production in PF1 of Áidejávri, the only layer showing biogenic CH₄ production during initial anoxic incubation was inhibited by stirring. High-resolution CH₄ kinetics of the non-stirred sample were markedly sigmoid (Fig. S1), suggesting that stirring could have inhibited growth of methanogens.

280



- 285 **Figure 7: Depth profiles of cumulative CH₄ production for permafrost cores at Iškoras, Áidejávri and Lakselv in loose anoxic incubations. (a) 96 days, (b) 350 days. CH₄ was corrected for desorption by subtracting CH₄ accumulating in oxic bottles from anoxic CH₄ release to obtain biogenic CH₄ production (Fig. S2). Anoxic PF2 from Áidejávri could not be measured after 350 days due to leakage. The active layer depths at the coring location were 60 cm (Iškoras and Lakselv) and 50 cm (Áidejávri).**
- 290 CH₄ production by thermokarst samples differed markedly from that of the corresponding layers in the permafrost cores (table 3). At Iškoras, CH₄ production in thermokarst cores was between 2 and 4 orders of magnitude larger than in corresponding samples from the intact permafrost core. Differences between thermokarst and corresponding permafrost layers were somewhat smaller for Áidejávri, but still pronounced. At both sites, CH₄ production was largest in the top layer of the thermokarst core (3 to 4 orders of magnitude larger than that in AL1
- 295 from the permafrost core), while CH₄ production of TK-PF1 and TK-PF2/3 at Áidejávri was in the same order of magnitude. In general, thermokarst samples responded more to oxygen and stirring/non-stirring than samples from the intact permafrost core, which makes it difficult to interpret differences between depths and sites (Fig. S9 and S10). Nevertheless, the potential to produce CH₄ increased dramatically in the former active layer peat when inundated (TK-AL) for both sites, illustrating the strongly increased methanogenetic potential of peat plateau AL
- 300 peat after thermokarst formation.



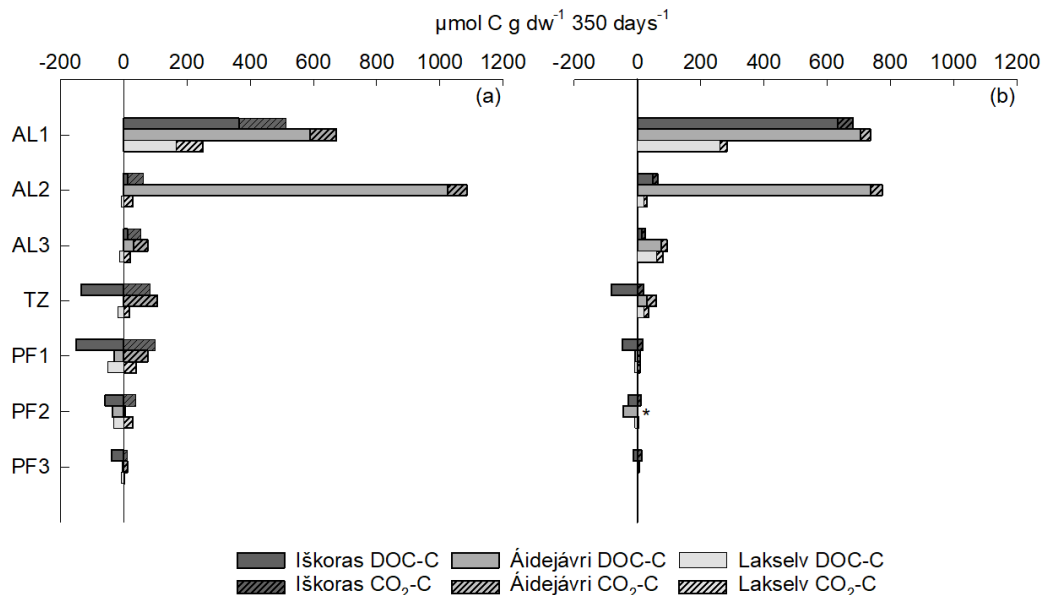
305 **Table 3: Comparison of cumulative CH₄ production (96 days) in loose anoxic incubations of permafrost core and thermokarst core samples at Áidejávri and Iškoras. The different layers of the thermokarst core are compared to corresponding layers in the permafrost core (AL1, PF1 and PF2/PF3) as shown in Fig 1. PF2 was used as the deep permafrost sample at Áidejávri because of mineral soil in PF3. For absolute depths, see table S1 and S2.**

nmol CH ₄ g dw ⁻¹ 96 days ⁻¹					
Permafrost core			Thermokarst core		
	Iškoras	Áidejávri		Iškoras	Áidejávri
			New peat		335
AL1	3	3	TK-AL	19661	7014
PF1	44	159	TK-PF1	1824	77
PF2/PF3	5	49	TK-PF2/3	3127	262

3.5 Total C mobilisation

310 Net release of DOC throughout incubation, measured as difference between initial and final extractable DOC, greatly exceeded CO₂-C release in loosely packed permafrost core samples (Fig. 8). Initially oxically incubated samples (Fig. 8a) had markedly smaller DOC, but larger CO₂-C production than anoxically incubated samples (Fig. 8b) and *vice versa*. pH increased more in anoxic incubations (table S10 and S11) which might have made DOC more easily extractable. When combining DOC and CO₂-C release, total C mobilisation was largest in the active layer irrespective of initial O₂ status. AL2 from Áidejávri showed very high C mobilisation compared with Iškoras and Lakselv. TZ and PF samples showed a tendency of net DOC consumption, which was most pronounced in samples from Iškoras.

315





320 **Figure 8: Combined CO₂-C production and net DOC release/uptake throughout ~350 days of incubation at 10 °C. Data from loosely packed permafrost core samples (a) incubated initially oxically and (b) anoxically. * no CO₂ data available due to leakage.**

4 Discussion

The cumulative CO₂ and CH₄ production showed a distinct depth pattern for permafrost cores at all three sites. The highest CO₂ production was found in the top of the active layer, in the transition zone and in the top of the permafrost. This suggests that peat from thawed permafrost peat has a considerable potential for CO₂ production, comparable with this of active layers. By contrast, CH₄ production under anoxic conditions was almost exclusively found in thawed permafrost layers. So far, only few studies have investigated decomposition in decaying peat plateaus by comparing post-thaw CO₂ production in thawed permafrost peat with that of overlaying active layers (Treat et al., 2014; Waldrop et al., 2021; Kirkwood et al., 2021; Harris et al., 2023).

Similar to the present study, Kirkwood et al. (2021) found the highest CO₂ release in the top of the active layer for Canadian peat plateaus (see Supplement, Kirkwood et al. (2021)) and for some sites a second maximum in the permafrost peat. To better compare the decomposition dynamics of the active layer and the permafrost, an average was calculated, showing similar trend in both studies with the active layer having higher potential degradation in anoxic incubations. The anoxic CO₂ accumulations in the active layer and permafrost peat reported by Kirkwood et al. (2021) were similar to the rates reported for Lakselv when adjusted for temperature and length of incubation (table S7). Both Iškoras and Áidejávri featured higher CO₂ production in the active layer and permafrost peat (table S7) than the average reported by Kirkwood et al. (2021). This could indicate a higher C degradability at our sites in Northern Norway compared to the Canadian sites.

Conversely, Treat et al. (2014) and Waldrop et al. (2021) did not observe any difference in C degradation between different depths at Alaskan peat plateaus. However, these studies differed in peat stratigraphy from our study. Furthermore, the degradation potentials were higher than those found in the present study (table S8 and S9). Harris et al. (2023) found that C degradation at Canadian peat plateaus was highest in the top of the active layer and that deeper layers had low CO₂ production throughout. These variations could be due to differences in carbon quality among the different sites, or due to differences in sample treatment.

In general, it is difficult to compare C degradation across published studies, because incubation conditions differ and information about peat formation and quality is lacking. The present study shows, however, that three peat plateaus situated within the same geographical region can differ greatly in peat quality and degradability. At the same time, this shows that more studies are required to estimate the potential carbon degradation in thawing permafrost peat. A standardised protocol for incubation experiments would improve the comparability among studies.

4.1 Constraints and variability in C decomposition

Oxygen availability was one of the main constraints for carbon decomposition, with CO₂ accumulation in anoxic incubations reaching only 7 % to 61 % of that in oxic incubations after 350 days. This is in agreement with other studies which found that O₂ availability is critical for CO₂ production after permafrost thaw (Estop-Aragones et al., 2018; Schädel et al., 2016). The incubation study by Waldrop et al. (2021) with arctic Alaskan peat found that



CO₂ accumulation after 6 months at 5°C under anoxic conditions accounted for 26% of that measured under oxic conditions. However, initially oxic conditions did not appear to increase subsequent anoxic C degradation.

The constantly stirred slurries were included to overcome diffusional constraints and to ensure full O₂ and substrate availability for aerobic and anaerobic metabolism. As expected, constant stirring of slurries increased CO₂ production and O₂ consumption as compared to loosely placed peat in the first phase of incubation. However, the addition of water to the slurries decreased the head space volume which meant that the absolute amount of O₂ present in the oxic slurries was smaller than in the oxic incubations with loose peat. The smaller amount of O₂ and the higher O₂ consumption in constantly stirred incubations resulted in slurries experiencing O₂ limitation earlier than loose incubations. Otherwise, differences in cumulative CO₂ production between loosely packed samples and slurries were relatively small (Fig. S3).

Cumulative CO₂ production of TZ and PF samples comparable to that of active layers suggests that carbon quality does not limit microbial decomposition of permafrost peat after thawing, despite having been frozen for centuries. This was true for all three sites despite marked variations in peat decomposability among the sites. The common depth pattern in degradability could be related to similar formation history of the three studied peat plateaus. The top of the active layer, where the highest rates were measured, includes the root zone with continuous input of fresh plant litter. This was also reflected in high C/N and δ¹³C values in this layer at all three sites. In the lower parts of the active layer, the peat has likely been exposed to aerobic conditions for decades or even centuries, without input of fresh plant litter. It may therefore be strongly decomposed and thus depleted of labile C which would explain the lower observed degradation rates for AL2 and AL3 layers. On the other hand, the PF layers contain frozen peat produced under wetland (i.e. mostly anaerobic) conditions which has not been exposed to decomposition since. Here, more labile C may still be available which could explain the secondary peak in degradation rates observed for the TZ and PF1 samples. Another explanation to why carbon degradation varied over depth at Áidejávri and Lakselv could be the increase in iron over depth (Fig. S4), which can trap organic C and limit mobilisation and degradation (Patzner et al., 2020). However, this cannot explain C degradation at Iškoras since this site overall has very little iron (Fig. S4).

Differences in C decomposition potentials between the sites might also be explained by difference in formation history or site-specific environmental factors. A study in a Swedish peat plateau found that reductive dissolution of iron during permafrost thaw can lead to increase in CH₄ emissions (Patzner et al., 2022). This might explain why Lakselv and Áidejávri, both having high iron contents, had a faster increase in CH₄ production compared to Iškoras having very little iron (Fig. S4).

4.2 Total C mobilisation

Initially oxic samples from all sites did not produce CH₄ for 350 days, indicating that methanogenesis was inhibited beyond the depletion of O₂ (Fig. S5, S6, S7). Yet, it cannot be ruled out that longer incubation time could have resulted in CH₄ production. DOC was consumed to a larger degree in initially oxic than anoxic PF samples (Fig. 8). This may be partly due to less DOC degradation under anoxic conditions, or it could be related to the higher extractability of DOC at higher pH in anoxic samples (Table S10 and S11).

In incubations of thawed cores from a Finnish peat plateau, Panneer Selvam et al. (2017) found that DOC from the active layer had a lower initial degradation potential than DOC from thawed permafrost. This agrees with the finding in the present study, that CO₂ accumulation in permafrost samples was faster than in deeper active layer



400 samples despite releasing less DOC, suggesting that ‘old’ permafrost DOC was more degradable than ‘new’ DOC in the active layer. This trend was especially evident at Áidejávri where CO₂ accumulation in the top permafrost exceeded that of the top active layer, despite releasing more DOC in the active layer. Still, the substantial release of DOC from the active layer is of concern because DOC is easily lost along water paths and can potentially increase the CO₂ production downstream (Panneer Selvam et al., 2017; Voigt et al., 2019).

Differences in gas kinetics for both CO₂ and CH₄ among the three peat plateaus could be related to differences in abundance and taxonomic composition of microbial communities. We tried to work aseptically during field sampling and laboratory sample handling, but cross-contamination (e.g. by the corer) cannot be excluded. Notwithstanding, our results suggest that permafrost samples harbour competent microbial taxa which proliferate over time as seen by the exponential product accumulation in some of our incubations. An incubation study with permafrost soil from the Tibetan Plateau found that CO₂ release after thawing showed a positive relationship with functional gene abundance for C degradation (Chen et al., 2020) without changing the composition of the microbial community. In general, high-altitude ecosystems differ from high-latitude ecosystems by having lower contents of OM and ice, with consequences for microbial community composition (Wang and Xue, 2021). In the present study, there were clear differences in the kinetics of gaseous product accumulation, both for CO₂ and CH₄. Thawed permafrost peat from Iškoras supported exponential CO₂ accumulation and PF peat from Áidejávri exponential CH₄ accumulation, strongly indicating microbial growth which will eventually result in community change. Detailed molecular studies would be needed to elucidate whether post-thaw community change leads to overall more degradation of permafrost C, or to a shift in the CO₂/CH₄ ratio under anoxic conditions.

415 **4.3 Thermokarst peat decomposition**

Inundation in thermokarst may be the ultimate fate of permafrost peat from decaying peat plateaus. It involves mixing with unfrozen peat, extended anoxia when inundated and buried by sediments and access to fresh C from autotrophic production in the ponds. Our results showed that the potential CO₂ production in the thawed permafrost was smaller in the thermokarst compared to the permafrost core. On the other hand, CH₄ production potentials over 96 days were several orders of magnitude higher than in undisturbed PF samples. This may be due to proliferation of a highly productive methanogenetic community over time, but also due to additional nutrient input from surrounding non-PF fens or bogs (In 'T Zandt et al., 2020).

The increase in CH₄ production seen after 350 days for the permafrost cores, especially at Lakselv and Áidejávri, suggests that proliferation of a functioning methanogenetic community after permafrost thaw takes time and depends, among others, on the fate of permafrost peat (e.g. inundation) after peat plateau collapse. This could mean that CH₄ production measured ex situ greatly underestimates the true CH₄ production potential of in situ thawed material, even in longer-term incubations. A similar conclusion can be drawn from the findings of Knoblauch et al. (2013) who incubated permafrost material from Holocene and Late Pleistocene permafrost sediments of the Lena River Delta in Siberia and found that CH₄ production reached maximum rates after an average of 2.6 years of incubation.

430 In our study, most CH₄ was produced by thermokarst peat from Iškoras; this could be related to the fact that permafrost thaw occurred more recently, with labile C still being present. The Áidejávri thermokarst site, on the other hand, has been thawed for a longer time which might explain why the C was more stable supporting less



methanogenesis. Another explanation might be differences in environmental factors such as soil moisture,
435 temperature and vegetation composition (Olefeldt et al., 2013).

Similar to our study, Kirkwood et al. (2021) incubated both peat plateau and thermokarst peat anoxically and
found higher CH₄ emissions in the thermokarst compared to active layer and permafrost samples after 225 days
(table S7). High pH was found to be a good predictor for potential CH₄ production in the Canadian thermokarst.
In our study, the opposite was the case; CH₄ production was highest in Iškoras thermokarst with lower pH than in
440 Áidejávri (table S5), suggesting that local differences in peat quality and time since thawing play a role for the
CH₄ emission potential.

5 Conclusion

This study quantified C degradability from active layer, transition zone and permafrost at three peat plateaus in
Northern Norway. In addition, samples from thermokarst adjacent to the peat plateaus were investigated at two of
445 the sites. Observed C degradation rates varied among the three sites, however, all three sites showed similar
degradation patterns over depth with largest CO₂ production in the top of active layer and a second maximum in
permafrost layers. Significant CH₄ production was only observed in samples from the transition zone and
permafrost layers after prolonged anoxic incubation. CH₄ production increased over time showing that
methanogenesis could play an important role in C degradation under prolonged anoxic conditions. This was
450 further supported by thermokarst samples that showed two and four orders of magnitude larger CH₄ production
rates as compared to peat plateau samples. DOC released during incubation of active layer peat plateau samples
exceeded that of CO₂-C and CH₄-C. Thus, when estimating C degradation in collapsing peat plateau ecosystems,
burial of permafrost peat in thermokarst and DOC runoff to down-stream ecosystems should be taken account for.

Data availability

455 Data are available on Zenodo <https://doi.org/10.5281/zenodo.10696561>.

Competing interests

The authors declare that they have no conflict of interest.

Acknowledgements

We would like to thank the laboratory staff at the Faculty of Environmental Sciences and Natural Resource
460 Management, NMBU, especially Trygve Fredriksen, Pia Frostad and Solfrid Lohne.



References

- Alewell, C., Giesler, R., Klaminder, J., Leifeld, J., and Rollog, M.: Stable carbon isotopes as indicators for environmental change in peatlands, *Biogeosciences*, 8, 1769-1778, <https://doi.org/10.5194/bg-8-1769-2011>, 2011.
- 465 Borge, A. F., Westermann, S., Solheim, I., and Etzelmüller, B.: Strong degradation of peatlands and peat plateaus in northern Norway during the last 60 years, *The Cryosphere*, 11, 1-16, <https://doi.org/10.5194/tc-11-1-2017>, 2017.
- Chen, Y., Liu, F., Kang, L., Zhang, D., Kou, D., Mao, C., Qin, S., Zhang, Q., and Yang, Y.: Large-scale evidence for microbial response and associated carbon release after permafrost thaw, *Global Change Biology*, 0, 1-12, <https://doi.org/10.1111/gcb.15487>, 2020.
- 470 Estop-Aragones, C., Cooper, M. D. A., Fisher, J. P., Thierry, A., Garnett, M. H., Charman, D. J., Murton, J. B., Phoenix, G. K., Treharne, R., Sanderson, N. K., Burn, C. R., Kokelj, S. V., Wolfe, S. A., Lewkowicz, A. G., Williams, M., and Hartley, I. P.: Limited release of previously-frozen C and increased new peat formation after thaw in permafrost peatlands, *Soil Biol Biochem*, 118, 115-129, <https://doi.org/10.1016/j.soilbio.2017.12.010>, 2018.
- 475 Harris, L. I., Olefeldt, D., Pelletier, N., Blodau, C., Knorr, K.-H., Talbot, J., Heffernan, L., and Turetsky, M.: Permafrost thaw causes large carbon loss in boreal peatlands while changes to peat quality are limited, *Global Change Biology*, 29, 5720-5735, <https://doi.org/10.1111/gcb.16894>, 2023.
- Hugelius, G., Loisel, J., Chadburn, S., Jackson, R. B., Jones, M., MacDonald, G., Marushchak, M., Olefeldt, D., Packalen, M., Siewert, M. B., Treat, C., Turetsky, M., Voigt, C., and Yu, Z.: Large stocks of peatland carbon and nitrogen are vulnerable to permafrost thaw, *Proceedings of the National Academy of Sciences*, 117, 20438-20446, <https://doi.org/10.1073/pnas.1916387117>, 2020.
- in 't Zandt, M. H., Liebner, S., and Welte, C. U.: Roles of Thermokarst Lakes in a Warming World, *Trends in Microbiology*, 28, 769-779, <https://doi.org/10.1016/j.tim.2020.04.002>, 2020.
- IUSS Working Group WRB: World Reference Base for Soil Resources 2014, update 2015. International Soil Classification System for Naming Soils and Creating Legends for Soil Maps, World Soil Resources Reports 106, 485
FAO, Rome, E-ISBN 978-92-5-108370-3, 2014.
- Kirkwood, J. A. H., Roy-Léveillé, P., Mykityczuk, N., Packalen, M., McLaughlin, J., Laframboise, A., and Basiliko, N.: Soil Microbial Community Response to Permafrost Degradation in Peatlands of the Hudson Bay Lowlands: Implications for Greenhouse Gas Production in a Warming Climate, *Global Biogeochemical Cycles*, 35, e2021GB006954, <https://doi.org/10.1029/2021GB006954>, 2021.
- 490 Kjellman, S. E., Axelsson, P. E., Etzelmüller, B., Westermann, S., and Sannel, A. B. K.: Holocene development of subarctic permafrost peatlands in Finnmark, northern Norway, *Holocene*, 28, 1855-1869, <https://doi.org/10.1177/0959683618798126>, 2018.
- Norsk Klimaservicesenter: <https://seklima.met.no/>, last access: 1 May 2021.
- 495 Knoblauch, C., Beer, C., Sosnin, A., Wagner, D., and Pfeiffer, E.-M.: Predicting long-term carbon mineralization and trace gas production from thawing permafrost of Northeast Siberia, *Global Change Biology*, 19, 1160-1172, <https://doi.org/10.1111/gcb.12116>, 2013.
- Lindgren, A., Hugelius, G., and Kuhry, P.: Extensive loss of past permafrost carbon but a net accumulation into present-day soils, *Nature*, 560, 219-222, <https://doi.org/10.1038/s41586-018-0371-0>, 2018.



- 500 Martin, L. C. P., Nitzbon, J., Scheer, J., Aas, K. S., Eiken, T., Langer, M., Filhol, S., Etzelmüller, B., and Westermann, S.: Lateral thermokarst patterns in permafrost peat plateaus in northern Norway, *The Cryosphere*, 15, 3423–3442, <https://doi.org/10.5194/tc-15-3423-2021>, 2021.
- Molstad, L., Dörsch, P., and Bakken, L.: Improved robotized incubation system for gas kinetics in batch cultures, 10.13140/RG.2.2.30688.07680, 2016.
- 505 Molstad, L., Dörsch, P., and Bakken, L. R.: Robotized incubation system for monitoring gases (O₂, NO, N₂O, N₂) in denitrifying cultures, *Journal of microbiological methods*, 71, 202–211, <https://doi.org/10.1016/j.jmimet.2007.08.011>, 2007.
- Obu, J., Westermann, S., Bartsch, A., Berdnikov, N., Christiansen, H. H., Dashtseren, A., Delaloye, R., Elberling, B., Etzelmüller, B., Kholodov, A., Khomutov, A., Kääb, A., Leibman, M. O., Lewkowicz, A. G., Panda, S. K.,
- 510 Romanovsky, V., Way, R. G., Westergaard-Nielsen, A., Wu, T., Yamkhin, J., and Zou, D.: Northern Hemisphere permafrost map based on TTOP modelling for 2000–2016 at 1 km² scale, *Earth-Science Reviews*, 193, 299–316, <https://doi.org/10.1016/j.earscirev.2019.04.023>, 2019.
- Olefeldt, D., Turetsky, M. R., Crill, P. M., and McGuire, A. D.: Environmental and physical controls on northern terrestrial methane emissions across permafrost zones, *Global Change Biology*, 19, 589–603, <https://doi.org/10.1111/gcb.12071>, 2013.
- 515 Panneer Selvam, B., Lapierre, J. F., Guillemette, F., Voigt, C., Lamprecht, R. E., Biasi, C., Christensen, T. R., Martikainen, P. J., and Berggren, M.: Degradation potentials of dissolved organic carbon (DOC) from thawed permafrost peat, *Scientific Reports*, 7, 45811, <https://doi.org/10.1038/srep45811>, 2017.
- Patzner, M. S., Mueller, C. W., Malusova, M., Baur, M., Nikeleit, V., Scholten, T., Hoeschen, C., Byrne, J. M.,
- 520 Borch, T., Kappler, A., and Bryce, C.: Iron mineral dissolution releases iron and associated organic carbon during permafrost thaw, *Nature Communications*, 11, 6329, <https://doi.org/10.1038/s41467-020-20102-6>, 2020.
- Patzner, M. S., Logan, M., McKenna, A. M., Young, R. B., Zhou, Z., Joss, H., Mueller, C. W., Hoeschen, C., Scholten, T., Straub, D., Kleindienst, S., Borch, T., Kappler, A., and Bryce, C.: Microbial iron cycling during permafrost collapse promotes greenhouse gas emissions before complete permafrost thaw, *Communications Earth & Environment*, 3, 76, <https://doi.org/10.1038/s43247-022-00407-8>, 2022.
- 525 Schädel, C., Bader, M. K. F., Schuur, E. A. G., Biasi, C., Bracho, R., Čapek, P., De Baets, S., Diáková, K., Ernakovich, J., Estop-Aragones, C., Graham, D. E., Hartley, I. P., Iversen, C. M., Kane, E., Knoblauch, C., Lupascu, M., Martikainen, P. J., Natali, S. M., Norby, R. J., O'Donnell, J. A., Chowdhury, T. R., Šantrůčková, H., Shaver, G. R., Sloan, V. L., Treat, C. C., Turetsky, M. R., Waldrop, M. P., and Wickland, K. P.: Potential carbon emissions dominated by carbon dioxide from thawed permafrost soils, *Nature Climate Change*, 6, 950–953, <https://doi.org/10.1038/nclimate3054>, 2016.
- Treat, C. C., Wollheim, W. M., Varner, R. K., Grandy, A. S., Talbot, J., and Frohling, S.: Temperature and peat type control CO₂ and CH₄ production in Alaskan permafrost peats, *Global Change Biology*, 20, 2674–2686, <https://doi.org/10.1111/gcb.12572>, 2014.
- 535 Treat, C. C., Natali, S. M., Ernakovich, J., Iversen, C. M., Lupascu, M., McGuire, A. D., Norby, R. J., Roy Chowdhury, T., Richter, A., Šantrůčková, H., Schädel, C., Schuur, E. A. G., Sloan, V. L., Turetsky, M. R., and Waldrop, M. P.: A pan-Arctic synthesis of CH₄ and CO₂ production from anoxic soil incubations, *Global Change Biology*, 21, 2787–2803, <https://doi.org/10.1111/gcb.12875>, 2015.



- 540 Turetsky, M. R., Wieder, R. K., Vitt, D. H., Evans, R. J., and Scott, K. D.: The disappearance of relict permafrost
in boreal north America: Effects on peatland carbon storage and fluxes, *Global Change Biology*, 13, 1922-1934,
<https://doi.org/10.1111/j.1365-2486.2007.01381.x>, 2007.
- Voigt, C., Marushchak, M. E., Mastepanov, M., Lamprecht, R. E., Christensen, T. R., Dorodnikov, M., Jackowicz-
Korczyński, M., Lindgren, A., Lohila, A., Nykänen, H., Oinonen, M., Oksanen, T., Palonen, V., Treat, C. C.,
Martikainen, P. J., and Biasi, C.: Ecosystem carbon response of an Arctic peatland to simulated permafrost thaw,
545 *Global Change Biology*, 25, 1746-1764, <https://doi.org/10.1111/gcb.14574>, 2019.
- Waldrop, M. P., McFarland, J., Manies, K. L., Leewis, M. C., Blazewicz, S. J., Jones, M. C., Neumann, R. B.,
Keller, J. K., Cohen, L., Euskirchen, E. S., Edgar, C., Turetsky, M. R., and Cable, W. L.: Carbon Fluxes and
Microbial Activities From Boreal Peatlands Experiencing Permafrost Thaw, *J Geophys Res-Bioge*, 126,
e2020JG005869, <https://doi.org/10.1029/2020JG005869>, 2021.
- 550 Wang, Y.-R., Hessen, D. O., Samset, B. H., and Stordal, F.: Evaluating global and regional land warming trends
in the past decades with both MODIS and ERA5-Land land surface temperature data, *Remote Sensing of
Environment*, 280, 113181, <https://doi.org/10.1016/j.rse.2022.113181>, 2022.
- Wang, Y. and Xue, K.: Linkage between microbial shift and ecosystem functionality, *Global Change Biology*, 0,
1-3, <https://doi.org/10.1111/gcb.15615>, 2021.

555